Role of Mast Cells in Early Epithelial Target Cell Injury in Experimental Acute Graft-Versus-Host Disease

George F. Murphy, Hirohiko Sueki, Cory Teuscher,† Diana Whitaker, and Robert Korngold*

Department of Dermatology, University of Pennsylvania School of Medicine, Philadelphia; *The Department of Microbiology and Immunology, Jefferson Medical College, Philadelphia, Pennsylvania; and †The Department of Microbiology, Brigham Young University, Provo, Utah, U.S.A.

The skin is a major target organ for graft-versus-host disease (GVHD), the principal complication of allogeneic bone marrow transplantation. The purpose of the present study was to test whether mast cell degranulation might be related to early target cell injury in the development of acute GVHD. We employed two irradiated murine strain combinations, one in which disease was mediated by $CD4^+$ effector T cells (B10.D2 → DBA/2), and the other by $CD8^+$ effector T cells (B10.BR → CBA). As compared to controls, both models exhibited mast cell degranulation of differing extents and patterns, as well as dyskeratosis in the epidermis before the influx of effector lymphocytes. These results suggested that factors produced and released by degranulated dermal mast cells might contribute to early target cell injury. Accordingly, the possible role of tumor necrosis factor (TNF)-α, a cytokine recently discovered in mast cell granules, was investigated by the injection of anti-TNF-α antibody during the course of disease mediated by either $CD4^+$ or $CD8^+$ T cells. Although overall survival of recipients undergoing $CD4^+$ T-cell-mediated GVHD was only slightly improved and the extent of mast cell degranulation was not affected by anti-TNF-α antibody treatment, the skin exhibited a significant diminution in the number of dyskeratotic cells/linear mm at 3-4 weeks post-transplantation. In contrast, anti-TNF-α antibody failed to enhance survival or reduce the number of dyskeratotic cells in the skin during $CD8^+$ T-cell-mediated disease. Finally, to determine whether $CD8^+$ T-cell-mediated GVHD was at all dependent upon mast cell involvement, the C3H.SW → B6WW^V strain combination was utilized, in which recipients were genetically deficient in mast cells. Onset of GVHD was significantly delayed in B6WW^V mice and was clearly correlated to the appearance and increase of *de novo* mast cells at later time points. *Key words: mast cells/graft-versus-host disease/target cell injury. J Invest Dermatol 102:451-461, 1994*

Acute graft-versus-host disease (GVHD) is a major complication of allogeneic bone marrow transplantation, with the skin a primary target organ [1]. The immunopathogenesis of GVHD, however, is still largely unknown, and the precise nature of the effector cells and their functional activity resulting in epithelial damage remain controversial. It has been generally thought that in GVHD, cytotoxic donor T cells (primarily $CD8^+$, although $CD4^+$ cells potentially exhibit overlapping functional activity) may directly destroy host target cells that reside in lympho-hematopoietic organs, the liver, the gastrointestinal tract, and the skin [2,3]. Alternatively, alloreactive T cells may produce localized inflammatory responses by release of cytokines that either damage tissue directly or produce injury by activation of non-specific inflammatory cells secondarily recruited to the site [4-6]. A likely candidate cytokine for induction of epithelial injury and associated inflammation in GVHD is tumor necrosis factor α (TNF-α), which is present in the serum of experimental animals with GVHD at times of peak epithelial injury [4]. Moreover, anti-TNF-α antibodies almost entirely prevented the cutaneous and intestinal epithelial lesions with reduced overall mortality in a murine GVHD model [5,7].

At the cellular level, mast cells that normally populate subepithelial connective tissue (e.g., skin, oropharynx, esophagus) and mucosal lamina propia (e.g., gut) may play a role in GVHD pathogenesis because stimulated $CD4^+$ and $CD8^+$ T cells secrete cytokines, particularly interleukin (IL)-3, that affect mast cell growth, activation, and release of mediators [8,9]. Electron microscopy studies of mast cells in the skin of mice undergoing GVHD have indicated active secretion [10]. Although it is not clear to what extent the different types of mast cell mediators produced have a bearing on the development of disease, it is interesting to note that TNF-like factors can be produced by murine mast cells [11-13]. It has also been recently demonstrated that human dermal mast cells express TNF-α mRNA and that purified mast cells release more TNF-α protein through degranulation on a per-cell basis than endotoxin-stimulated monocytes [14]. In certain target cells, TNF-α has been shown to cause DNA fragmentation, which leads to programmed cell death, or apoptosis [15]. Murine recipients of the keratin 14 promoter-driven TNF-α transgene have epithelial necrosis similar to that seen in acute GVHD [16]. Therefore, it is possible that some of the early epithelial injury in experimental GVHD could result from local TNF-α released through mast cell-dependent pathways.

In experimental murine models, T cells are required for the development of lethal GVHD directed to multiple minor histocompatibility (H) antigens [17]. Previous investigations have indicated

Manuscript received March 11, 1993; accepted for publication December 2, 1993.

Reprint requests to: Dr. Robert Korngold, Department of Microbiology and Immunology, Jefferson Cancer Institute, Jefferson Medical College, 233 S. 10th Street, Philadelphia, Pennsylvania 19107.

Abbreviations: Ab, antibody; ATBM, anti-Thy-1-treated bone marrow; BSS, buffered saline solution; C, complement; CTMC, connective tissue mast cell; GVHD, graft-versus-host disease; H, histocompatibility; MST, median survival time; NK cell, natural killer cell; rER, rough endoplasmic reticulum.

0022-202X/94/$07.00

that either CD4+ or CD8+ T-cell subsets are capable of mediating GVHD across minor H barriers, depending upon the particular strain combination utilized [18,19]. With use of highly purified preparations of donor T-cell subsets, CD8+ T cells, by themselves, were capable of mediating lethal disease in all strain combinations tested (e.g., B10.BR → CBA), whereas CD4+ T cells were potent effectors in only two strain combinations, one of which is the B10.D2 → DBA/2 model [18]. Pathologic examination of skin lesions induced by minor H antigenic differences in these strain combinations has revealed these models to be 1) similar to cutaneous GVHD in humans, 2) quantifiable according to the number of dyskeratotic cells/mm of epidermis 3) related in severity to the number of T cells in the donor marrow inocula, and 4) accurate indicators of associated gastrointestinal and visceral disease [20–23].

In the present study, we utilized antibody-treated donor inocula to produce CD4+ and CD8+ T-cell–mediated GVHD and to characterize further sequential alterations by ultrastructural and quantitative analysis. Specifically, we attempted to clarify the role of mast cells and TNF in early epidermal injury and in subsequent effector cell recruitment during GVHD. Our results indicate that 1) degranulation of mast cells precedes vascular activation and subsequent influx of effector cells, 2) mast cells at early timepoints of CD4+ T and CD8+ T-cell–mediated GVHD display evidence of active degranulation or decreased numbers of granules, respectively, 3) whereas early epithelial target cell injury (day 7 post-transplantation) is unaffected by the anti–TNF-α antibody (Ab) treatment in both models, passive immunization significantly reduces dyskeratosis at 3–4 weeks post-transplantation in CD4+ T-cell–mediated GVHD but not in disease mediated by CD8+ T cells, and 4) transplantation of C3H.SW CD8+ effector T cells into irradiated mast cell–deficient B6W/W^V mice results in significantly delayed development of GVHD pathologic changes when compared to control B6+/+ recipients, indicating a dependency upon mast cells for the development of CD8+ T-cell–mediated epithelial injury. Taken collectively, these data suggest that mast cells may participate both directly and indirectly in the early pathogenesis of acute experimental GVHD.

MATERIALS AND METHODS

Animals B10.BR/SgSn, B10.D2/oSnJ, CBA/J, C3H.SW/SnJ, DBA/2J, WBB6F_1/J-W/W^V (B6W/W^V), and WBB6F_1/J+/+ (B6+/+) mice were purchased from the Jackson Laboratory (Bar Harbor, ME). Male mice were used as cell donors between 7 and 12 weeks of age and as recipients between 9 and 16 weeks of age. Mice were always kept in a sterile environment in microisolator cages (Lab Products, Maywood, NJ) and provided with autoclaved food and acidified water (pH 2.5).

Monoclonal Antibodies (MoAbs) Ascites fluid for anti–Thy-1.2 (J1j, rat immunoglobulin [Ig]M [24]), anti-CD4 (GK1.5, rat IgG2a [25], and RL172, rat IgM [26]), anti-CD8 (3.168, rat IgM [27]), and supernatant from anti–B-cell (J11d; rat IgM [24]) MoAbs were used for cell preparations. Guinea pig serum was used as a source of complement (C) for all MoAb treatments.

Preparation of Rabbit Antisera Rabbit anti–TNF-α antiserum and control rabbit IgG were prepared according to previously described protocols [28]. In brief, five female New Zealand white rabbits (2–3 kg) were immunized with 50 mg of recombinant murine TNF-α emulsified in complete Freund's adjuvant (CFA) supplemented with *M. tuberculosis* (H37Ra) at a concentration of 9 mg/ml. This emulsion was distributed intradermally (i.d.) among 10–12 sites on the back of each rabbit. All animals were boosted subcutaneously with 10 mg of recombinant murine TNF-α in incomplete Freund's adjuvant 20 d later and screened for the production of anti–TNF-α Abs using a solid-phase radioimmunoassay 30 d after the initial injection. All animals were found to be producing equivalent high titers of anti–TNF-α antibody and were bled serially. Two rabbits were immunized with CFA and an irrelevant antigen. Their pooled serum served as the source of the control IgG. Rabbit anti-CFA IgG (CFA RIgG) and anti-murine TNF-α IgG were purified by protein A sepharose (Pharmacia, Piscataway, NJ) affinity chromatography. The specificity of the anti–TNF-α Ab preparation was characterized by Western blot analysis. CFA RIgG control serum pools failed to demonstrate immunoreactivity with murine TNF-α in Western blots. In contrast, the anti–TNF-α antiserum pool exhibited specific immunoreactivity with the immunogen. The efficacy of the purified anti–TNF-α IgG at blocking the biologic responses mediated by TNF-α was assessed in endotoxin protection assays as described previously [28].

Preparation of Donor Cells Donor cells were prepared according to previously described protocols [18]. In brief, bone marrow cells were obtained from the femurs and tibiae of donor mice by flushing with buffered saline solution (BSS) supplemented with 0.1% bovine serum albumin (BSA; Hyclone, Logan, UT). To prepare anti–Thy-1–treated (T-cell–depleted) bone marrow (ATBM), cells were incubated with J1j MoAb (diluted 1:100) and complement (C) (1:25) for 45 min at 37°C, followed by four washes. T-cell–enriched donor cell populations were prepared by treating pooled spleen and lymph node cells with the anti–B-cell J11d MoAb (diluted 1:5) and C (1:25) for 1 h at 37°C. This treatment generally resulted in a population of between 90 and 95% Thy1+ cells, as measured for phenotyping by flow cytometric analysis.

For preparation of purified T-cell subset populations, as described elsewhere [18], J11d plus C-treated lymphocytes were further treated with appropriate MoAb and C directed against the undesirable subset. For example, to purify CD4+ T cells, lymphocytes were treated twice with anti-CD8 MoAb (3.168; diluted 1:50) plus C (1:25) for 45 min at 37°C, initially, and again for 30 min with a wash in between. After another wash, the cells ($< 1.5 \times 10^8$) were placed on a Petri plate (150 mm, Falcon non-tissue culture grade) coated with GK1.5 anti-CD4 MoAb (preincubated for 1 h at room temperature with 15 ml of a 1:12,000 dilution of ascites fluid) in a volume of 8 ml BSS and kept stationary at 4°C for 1 h. Nonadherent cells were poured off and the plate was washed 5–6 times by gentle swirling and pouring. Adherent CD4+ cells were then eluted by forceful pipetting. An analogous procedure was used to prepare purified CD8+ T cells, with the substitution of a single RL172 anti-CD4 MoAb plus C treatment, and a 30-min incubation on ice of the cells with the anti-CD8 MoAb (1:50 dilution) alone. Cells were then washed once and positively panned on a plate coated with goat anti-rat IgM Ab (preincubated with 1:200 dilution; Cooper Biomedical, Malvern, PA). Eluted subsets were phenotyped by flow cytometry analysis and were routinely found to be negative for the opposite subset.

GVHD Induction The B10.D2 → DBA/2 (900 cGy) strain combination was used for studies with CD4+ T-cell–mediated GVHD, whereas the B10.BR → CBA (800 cGy), C3H.SW → B6W^V (850 cGy), and C3H.SW → B6+/+ (850 cGy) strain combinations were used for studies with CD8+ T-cell–mediated GVHD. Recipient mice were irradiated with the appropriate exposure from a Gammacell 137Cs source (130 cGy/min). Approximately 6 h later, these recipients were injected intravenously with donor cells *via* the tail vein. The inoculum consisted of either ATBM cells (2×10^6) alone as a negative control, or a mixture of ATBM (2×10^6) together with either donor-purified CD4+ or CD8+ T cells (with dosage between 2 and 4×10^6 cells, depending upon the particular strain combination). Irradiated recipient mice were passively immunized by an initial intravenous injection of rabbit anti-mouse TNF-α Ab (2 mg) or control CFA RIgG, within 5 h after irradiation and 1 h before transplantation. Ab was then administered intraperitoneally (2 mg) on a weekly basis for up to 6 weeks post-transplantation. Mice, which were treated with neither anti–TNF-α Ab nor CFA RIgG, served as positive controls. Mortality was observed daily for between 80 and 100 d.

Biopsy Serial ear biopsies were performed on six animals (CD4+ effector series) or three animals (CD8+ effector series) for each experimental condition at each timepoint, beginning at the time of transplantation (day 0) and sequentially every 7 d thereafter until death or a maximum of 42 d. Biopsies were full thickness, measured 3×2 mm, and were taken from alternating sides. Attention was paid to avoid previous healing surgical wounds.

Light and Electron Microscopy The specimens were immediately fixed in 4% glutaraldehyde overnight and then rinsed with 0.1 M sodium cacodylate buffer (pH 7.4). Tissues were postfixed with 2% osmium tetroxide for 2 h, dehydrated in graded ethanol, and embedded in Epon 812. One-micron–thick sections were cut with a Porter-Blum MT2B ultramicrotome, stained with toluidine blue, and finally dipped in 95% ethanol for light microscopic analysis.

The number of dyskeratotic epidermal cells/linear mm, which has been previously shown to correlate with disease severity and with number of transplanted T cells in this model of GVHD [21,23], was counted under a ×100 objective and a ×10 eyepiece of a light microscope. More than 10 linear mm of the epidermis was assessed in each animal and at each timepoint. Extent of mast cell degranulation was also evaluated under the same magnification, as follows: category I, < 25% of granules depleted; category II, 25–75% of granules depleted; and category III, > 75% of granules depleted. Fully granulated mast cells, as defined by control skin, showed cyto-

plasmic area to be entirely filled with darkly stained metachromatic granules. Granule depletion was evidenced by loss of metachromasia over portions of the cytoplasmic area. Because hypogranular mast cells could also represent dying or degenerating cells, confirmation of active degranulation and absence of degenerative alterations were established by transmission electron microscopy. More than 40 mast cells were evaluated in each animal and at each timepoint. Ear thickness, which paralleled the extent of dermal infiltration by leukocytes, was measured 1 mm beneath the top of the ear.

For electron microscopy, ultrathin sections were cut with a Porter-Blum MT2B ultramicrotome. Sections were stained with uranyl acetate and bismuth, and observed in a Hitachi H-7000 electron microscope.

Statistical Analysis Data were pooled from two separate experiments and involved the analysis of skin samples from between three and eight mice at each timepoint for the determination of the number of dyskeratotic cells per mm, extent of mast cell degranulation, and ear thickness. Significant differences between experimental groups were determined using Fisher's least-significant difference test for the multiple analysis of variance. The GVHD mortality assays represented pooled data from two to three separate experiments and involved a total of 14–18 mice per group, and median survival time (MST) values were statistically compared by Wilcoxon nonparametric rank analysis.

RESULTS

Biopsies from control recipients of T-cell–depleted ATBM showed only small numbers of perivascular leukocytes and only rare exocytotic lymphoid cells and dyskeratotic epidermal cells. In contrast, skin from both $CD4^+$ (B10.D2 → DBA/2 900 cGy) and $CD8^+$ (B10.BR → CBA 800 cGy) cell-mediated GVHD models demonstrated a defined sequence of pathologic changes consisting of progressive leukocyte infiltration and dyskeratosis typical of cutaneous acute GVHD [23]. Leukocytes first appeared about superficial dermal vessels between days 14 and 21 post-transplantation, and epidermal dyskeratosis and leukocyte exocytosis became prominent between days 21 and 35.

Early Alterations in GVHD: Days 0–7 The first pathologic alteration observed by light or electron microscopy in either strain combination occurred at day 7 and consisted of evidence of mast cell degranulation in $CD4^+$ cell-mediated disease (Fig 1) and hypogranulated mast cells without evidence of active degranulation in $CD8^+$ cell-mediated GVHD (Fig 2). Skin in both strain combinations at this juncture was devoid of leukocyte influx. Hypogranular mast cells in $CD8^+$ cell-mediated GVHD showed no evidence of cytoplasmic or nuclear degeneration by ultrastructure, suggesting that their state of degranulation was the result of previous granule discharge and not due to degenerative alterations. In both $CD4^+$ and $CD8^+$ cell-mediated disease, epidermal cells showed dyskeratosis in association with mast cell degranulation or hypogranulation. By kinetic analysis, the number of dyskeratotic cells per mm of skin increased equivalently over the time course of the study for both $CD4^+$ (Fig 3*b*) and $CD8^+$ (Fig 4*b*) cell-mediated GVHD, without statistical significance between disease caused by either donor T-cell subset ($0.29 < p < 0.98$). In contrast, marked differences between donor T-cell subsets were observed in the extent of mast cell degranulation by light microscopy, particularly on day 7 post-transplantation (Figs 3*c* and 4*c*). Significantly more mast cells consistent with level II (involving 25–75% granule depletion; approximately a 2× increase; $p < 0.04$) and level III (involving > 75% granule depletion; approximately a 3× increase; $p = 0.03$) were evident in the $CD4^+$ cell-mediated group (Fig 3*c*) as compared to the $CD8^+$ cell-mediated group (Fig 4*c*). In addition, the percentage of mast cells of $CD8^+$ cell-mediated GVHD, consistent with level I (involving <25% granule depletion), was significantly higher than that of $CD4^+$ cell-mediated disease ($p < 0.01$).

Leukocyte Infiltration in $CD4^+$ and $CD8^+$ Cell-Mediated GVHD: Days 14–35 Influx of leukocytes into the skin, observed with either strain combination, was first noted on day 14 post-transplantation. Lymphocytes containing membrane-bound electron-dense cytoplasmic granules were observed within the dermal microvessels (Fig 2*C*, *D*). Endothelial cells were enlarged and protruded into the vessel lumens, indicative of "activation." Occasional lymphocytes adhered to endothelial cells and were penetrating microvessels. Diapedesis of lymphocytes attained maximum levels at days 21–35.

In $CD4^+$ cell-mediated GVHD, neutrophils accumulated within lumens of microvessels prior to accumulation of lymphocytes. Neutrophils predominated in microvessels at day 14, whereas the population of intralumenal lymphocytes gradually increased after day 14. In contrast to $CD4^+$ cell-mediated GVHD, intralumenal neutrophils were consistently absent in $CD8^+$ cell-mediated disease at the timepoints examined (Fig 2*C*).

Lymphocytes with or without membrane-bound dense granules migrated into the epidermis (exocytosis) in both $CD4^+$ and $CD8^+$ cell-mediated GVHD. These lymphocytes, along with dendritic monocytes devoid of Birbeck granules, frequently surrounded dyskeratotic keratinocytes (satellitosis). Many dyskeratotic cells, however, were unassociated with exocytotic lymphocytes in the sections examined (Figs 2*D* and 5). The combined results for ultrastructural changes in $CD4^+$ T-cell–mediated versus $CD8^+$ T-cell–mediated GVHD are summarized in Table I.

Effect of Anti–TNF-α Ab on GVHD Mediated by $CD4^+$ T Cells Irradiated DBA/2 mice transplanted with 2×10^6 B10.D2 ATBM cells and 2×10^6 purified $CD4^+$ T cells without Ab treatments exhibited an incidence of lethal GVHD of 60% with a median survival time (MST) of 40 d (Fig 3*a*). Similarly, transplanted mice injected weekly with 2 mg of CFA RIgG had 69% mortality and a MST of 36 d. In contrast, transplanted mice treated with weekly injections of 2 mg of anti–TNF-α Ab exhibited significantly improved survival with 39% incidence of lethal GVHD and a MST of > 100 d ($p = 0.05$ in comparison to the untreated group and $p < 0.01$ compared to the CFA RIgG-treated group). Survival of the anti–TNF-α Ab-treated recipients was also significantly below the complete survival of DBA/2 mice transplanted with 2×10^6 B10.D2 ATBM cells alone ($p < 0.01$), indicating that TNF-α activity by itself was not likely to be the only factor responsible for GVHD mortality.

As anticipated, treatment with anti–TNF-α Ab did not significantly affect the degree of dermal mast cell degranulation (a presumed source of some of the locally produced TNF-α), which is observed at early timepoints (days 7 and 14) after B10.D2 $CD4^+$ T-cell transplantation in untreated DBA/2 mice ($0.06 < p < 0.92$) (Fig 3*c*). In regard to the kinetic development of dyskeratotic cells found in the skin (Fig 3*b*), untreated mice undergoing $CD4^+$ T-cell–mediated GVHD exhibited significantly greater numbers of dyskeratotic cells/mm than mice receiving ATBM alone on days 7, 21, 28, and 35 post-transplant ($p < 0.01$), and did not differ from mice administered control CFA RIgG ($0.17 < p < 0.93$). On the other hand, skin from animals treated with anti–TNF-α Ab between days 14 and 28 exhibited similar numbers of dyskeratotic cells to that of the ATBM control group and was significantly lower in comparison to untreated mice undergoing $CD4^+$ T-cell–mediated GVHD on days 21, 28, and 35 ($p < 0.01$).

The mean ear thickness in untreated DBA/2 mice transplanted with B10.D2 $CD4^+$ T cells was significantly greater than that of mice given ATBM alone on days 21 and 35 ($p < 0.01$) post-transplantation (Fig 3*d*). In contrast, the ear thickness in anti–TNF-α Ab-treated recipients was significantly diminished from the untreated group on days 21 and 35 ($p < 0.01$), but not different from the ATBM control at any timepoint ($0.24 < p < 0.95$). Treatment of mice with CFA RIgG failed to diminish the ear thickness significantly from the untreated control at any timepoint ($0.07 < p < 0.50$).

Effect of Anti–TNF-α Ab on GVHD Mediated by $CD8^+$ T Cells Irradiated (800 cGy) CBA mice transplanted with 2×10^6 B10.BR ATBM cells and 2.5×10^6 purified $CD8^+$ T cells without Ab treatments exhibited an incidence of lethal GVHD of 67% with a MST of 37 d (Fig 4*a*). Similarly transplanted mice injected weekly with 2 mg of CFA RIgG had 75% mortality and a MST of 31 d. Recipient mice treated with weekly injections of 2 mg of anti–

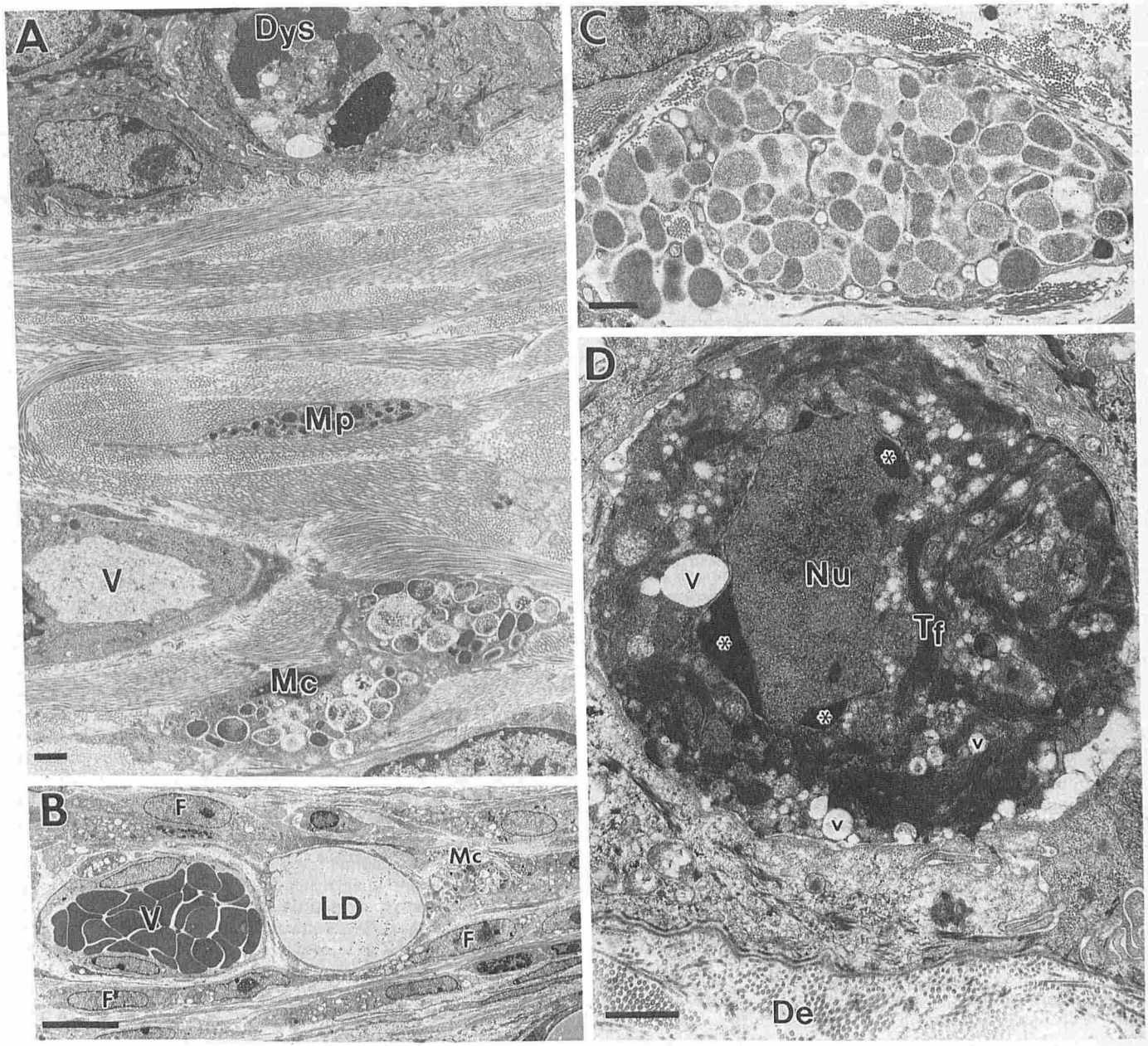

Figure 1. Electron micrographs of early alterations (day 0–7) in B10.D2 → DBA/2 $CD4^+$ cell-mediated GVHD. *A)* The initial events in $CD4^+$ cell-mediated disease were extensive degranulation of mast cells (Mc) and dyskeratosis (Dys), without evidence of influx of effector cells. V, microvessel; Mp, melanophage (*bar,* 1 μm). *B)* Neither lymphocytes nor neutrophils were accumulated within the vessel (V) in this phase, although mast cells (Mc) were consistently degranulated. F, fibroblast; LD, lipid droplet (*bar,* 10 μm). *C)* Mast cells exhibited complete degranulation, characterized by granule enlargement, membrane fusion of adjacent granules and between granule and plasma membranes, and electron lucency of granule matrices (*bar,* 1 μm). *D)* Dyskeratotic cells were mainly concentrated on the basal cell layer. The nuclear chromatin of dyskeratotic cells was homogeneously aggregated *(asterisks).* Numerous vacuoles (V) were interspersed among abnormally condensed tonofilaments (Tf). Nu, nucleus; De, dermis (Bar, 1 μm).

TNF-α Ab failed to show amelioration of mortality with 83% incidence of lethal GVHD and a MST of 29 d ($p = 0.21$ in comparison to CFA RIgG treatment). Moreover, when compared to the untreated mice, anti-TNF-α Ab administration could not significantly decrease the number of dyskeratotic cells at any measured timepoint 7–28 d post-transplantation ($0.27 < p < 0.99$) (Fig 4*b*). Treatment with CFA RIgG also did not significantly affect the number of dyskeratotic cells, except at day 35 ($p = 0.02$). An analysis of the percentage of mast cells degranulating and of the extent of degranulation did not reveal any significant differences between the untreated and anti-TNF-α Ab-treated transplant recipients at either 7 or 14 d after GVHD induction ($0.09 < p < 0.76$)(Fig 4*c*). Likewise, no significant differences were found in ear thickness between any of the experimental groups, except between untreated and either CFA RIg-treated or ATBM mice on day 7 ($p < 0.03$) (Fig 4*d*).

The sequential developments of ultrastructural changes in the skin were also similar between untreated $CD8^+$ T-cell-mediated GVHD-induced CBA mice and those treated with anti-TNF-α Ab. Anti-TNF-α Ab treatment did not influence the quality of mast cell degranulation, vascular activation, diapedesis of leukocytes, and the subsequent exocytosis of lymphocytes.

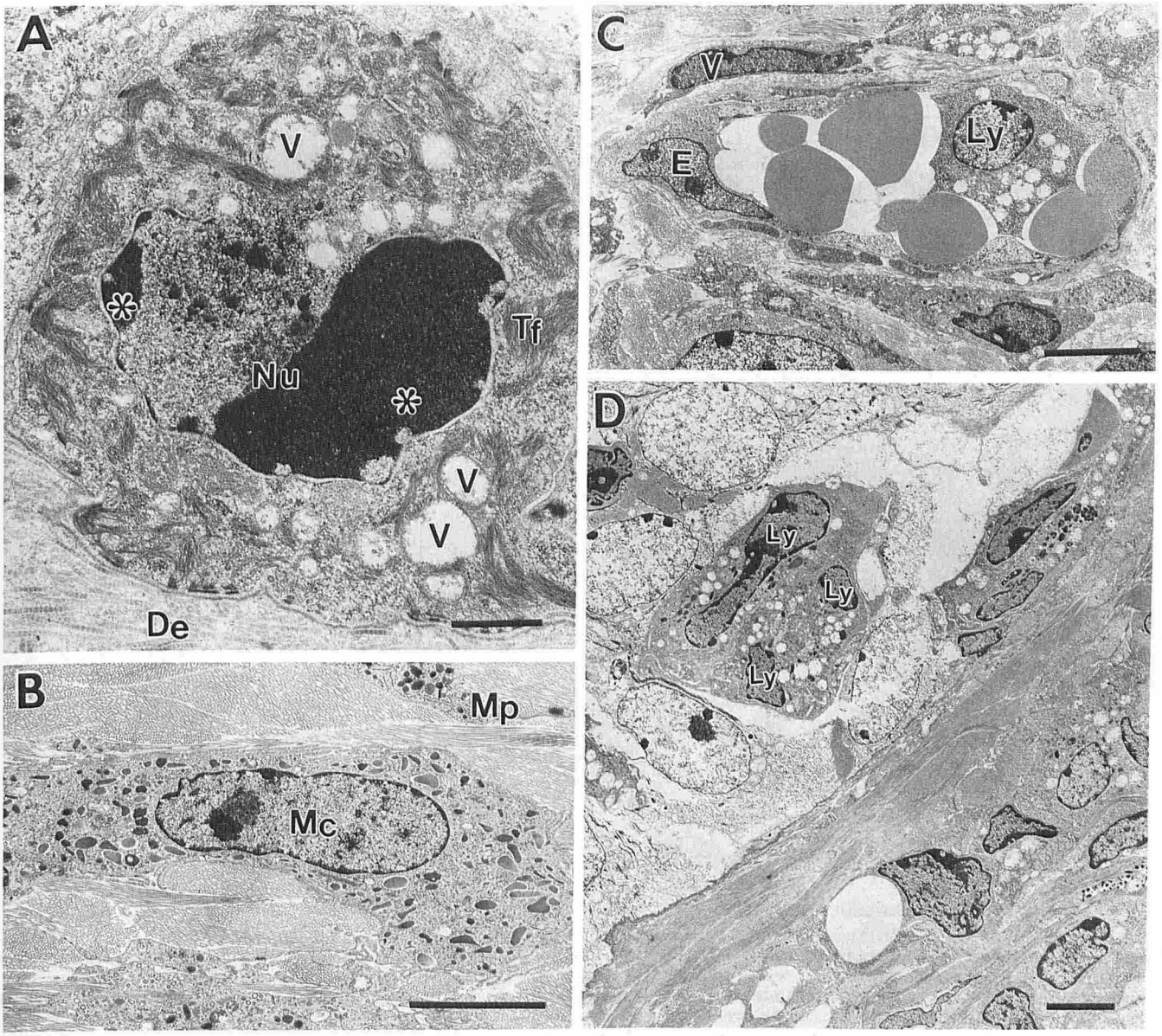

Figure 2. Sequential ultrastructure of early B10.BR→CBA CD8+ cell-mediated GVHD (day 0–7). Dyskeratosis and hypogranulation of mast cells preceded influx of effector lymphocytes in CD8+ cell-mediated disease. *A)* The ultrastructural features of dyskeratotic cells in CD8+ cell-mediated GVHD were identical to that in CD4+ cell-mediated disease. Nu, nucleus; *asterisks,* homogeneously aggregated nuclear chromatin; V, vacuoles; Tf, tonofilaments (*bar,* 1 μm). *B)* A hypogranulated mast cell (Mc) at day 7 of CD8+ cell-mediated GVHD, without evidence of active degranulation. Mp, melanophage (*bar,* 5 μm). *C)* Only lymphocytes (Ly), with or without membrane-bound dense granules, were accumulated within microvessels at day 14 of CD8+ cell-mediated GVHD. V, veil cell; E, endothelial cell (*bar* = 5 μm). *D)* The ultrastructure of exocytotic lymphocytes (Ly) often containing membrane-bound dense cytoplasmic granules in CD8+ cell-mediated GVHD was similar to that of CD4+ cell-mediated disease (*bar,* 1 μm).

Effect of Genetic Mast Cell Depletion on CD8+ T-cell–mediated GVHD B6WW^V and B6$^{+/+}$ mice were irradiated (850 cGy) and transplanted with 2×10^6 C3H.SW ATBM cells and 4×10^6 purified C3H.SW CD8+ T cells or with ATBM alone (Fig 6*a*). The incidence of GVHD mortality was moderate in both groups of recipients, with significantly greater survival in the B6WW^V recipients (50%, 96-d MST versus 30%, 60-d MST for B6$^{+/+}$ mice) ($p < 0.03$).

Sequential histopathologic analysis of skin samples from both B6WW^V and B6$^{+/+}$ mice undergoing development of GVHD indicated a marked diminution in the number of dyskeratotic cells/mm in the skin of B6WW^V recipients in comparison to B6$^{+/+}$ mice (Fig 6*b*). The differences were statistically significant on days 14, 21, and 28 post-transplantation ($p < 0.01$). The number of dyskeratotic cells in the skin of B6WW^V recipients of C3H.SW CD8+ T cells exhibited a gradual increase from day 21 on, reaching the level found in B6$^{+/+}$ recipients by day 40 ($p = 0.25$). The number of dyskeratotic cells in the skin of B6WW^V mice undergoing GVHD was significantly higher than B6WW^V mice given ATBM alone on day 40 ($p < 0.01$) and approached significance on both days 21 and 30 post-transplantation ($0.05 < p < 0.06$).

Ultrastructurally, at the time of transplantation (day 0), no definitive mast cells could be identified in the skin of B6WW^V recipients, although occasional mononuclear cells possibly representing mast cell precursors were observed around dermal microvessels (Fig 7*A*). These cells were characterized by oval nuclei, dendritic cytoplasmic processes, a number of poorly defined vesicles, cytoplasmic vacuoles that occasionally contained moderately electron-dense granular and

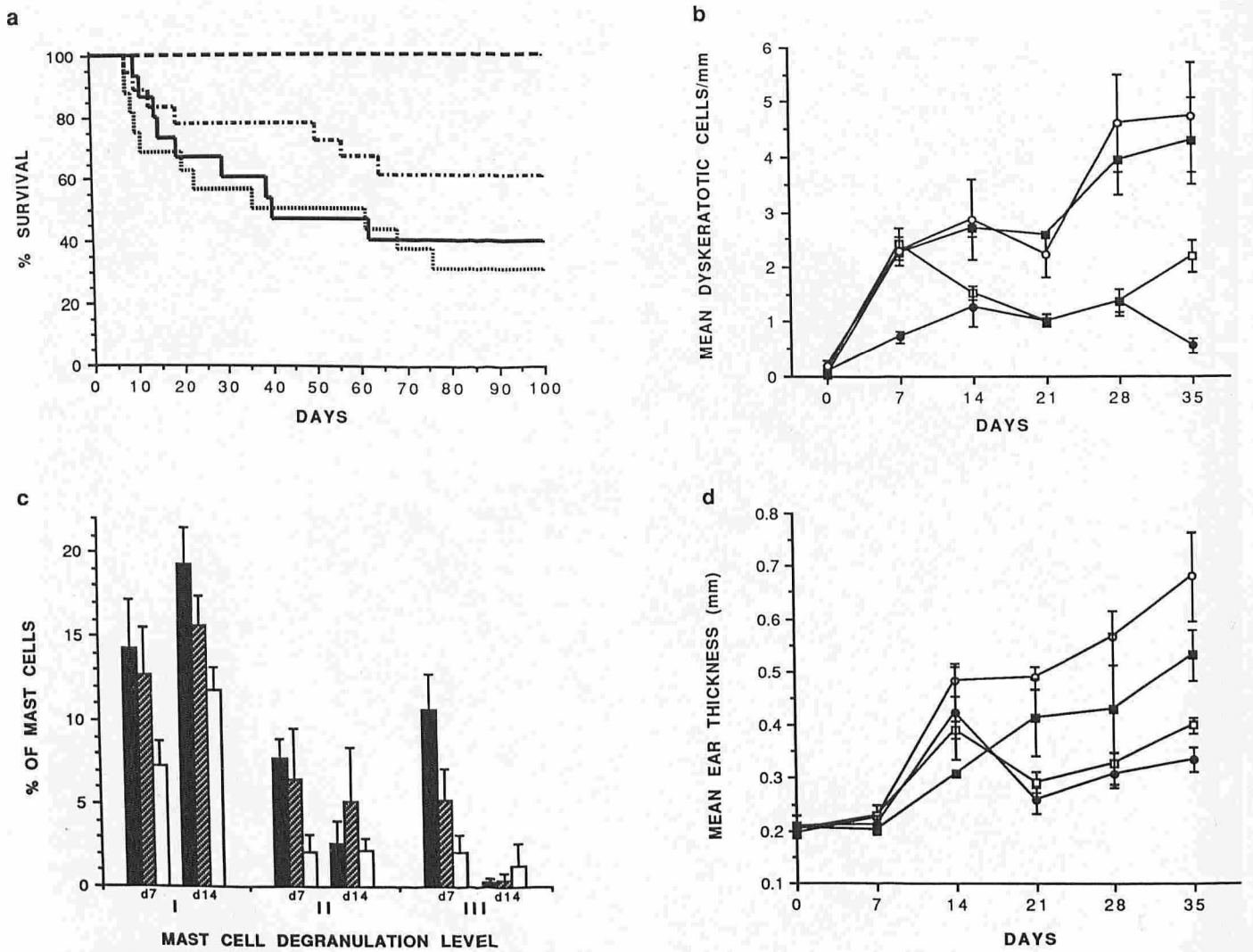

Figure 3. Effect of anti-TNF-α Ab treatment on development of CD4$^+$ T-cell-mediated GVHD. *a)* Survival and incidence of GVHD. DBA/2 mice were irradiated (900 cGy) and injected intravenously with either 2×10^6 B10.D2 ATBM cells alone (- - ; n = 14) or with 2×10^6 B10.D2 CD4$^+$ T cells. The latter mice were divided into three groups, the first left untreated (—— ; n = 15), the second given anti-TNF-α Ab (2 mg intravenously, 1 h before cells were injected; 2 mg intraperitoneally weekly thereafter till day 42) (-·-·-·- ; n = 18), and the third treated with control CFA RIgG (2 mg intravenously, 1 h before cells were injected; 2 mg intraperitoneally weekly thereafter until day 42) (····· ; n = 16). *b)* Sequential analysis of the mean ± SEM number of dyskeratotic cells/linear mm of skin from DBA/2 mice of the four groups described in (*a*) from days 0–35 post-transplantation; an average of n = 6 for untreated (○) and anti-TNF-α Ab (□), n = 3 for CFA RIgG (■), and n = 4 for ATBM (●). *c)* The mean ± SEM percentage of mast cells degranulating and the extent of degranulation in the skin of DBA/2 mice from the untreated (■; n = 7), anti-TNF-α Ab treated (▨; n = 6, d 7 and n = 5, d 14), and ATBM (□; n = 3) groups at days 7 and 14 post-transplantation. *d)* Sequential analysis of the mean ± SEM ear thickness from DBA/2 mice of the four groups described in *(b)* from days 0–35 post-transplantation (n = 3 for all groups and timepoints).

flocculent material, and fibronexus-like electron-dense plaques (Fig 7*B*). By day 14, these perivascular cells exhibited widening of rough endoplasmic reticulum (rER) and had developed increased numbers of moderately electron-dense granular matrices within membrane-bound cytoplasmic vacuoles (Fig 7*C*). By days 30–40, mast cell-like cells and occasional definitive mast cells containing granular matrices accompanied by electron-lucent halos were evident about superficial vessels (Fig 7*D*). These latter cells contained numerous electron-dense granules with some evidence of degranulation, characterized by granule enlargement, membrane fusion, and decreased electron density of granular matrices (Fig 7*D*).

The sequential ultrastructural appearance of mast cells in control B6$^{+/+}$ mice undergoing GVHD development were similar to those previously described for B10.BR → CBA CD8$^+$ T-cell-mediated disease. A small number of completely degranulated mast cells and a large number of mast cells with decreased numbers of granules, but without evidence of active degranulation, were observed on day 7 and day 14 in diseased B6$^{+/+}$ recipients. B6$^{+/+}$ transplant recipients exhibited dermal and epidermal accumulation of lymphocytes with associated sequential ultrastructural alterations that were indistinguishable from CD8$^+$ cell-mediated disease in the B10.BR → CBA combination. Transplanted B6*WW^V* mice, on the other hand, did not demonstrate similar cellular infiltrates and associated changes until days 30–40, indicating a delay in histologic evidence of disease, which coincided with the appearance of granulated mast cells.

DISCUSSION

This study was designed to address whether mast cells, or their cytokine products (TNF-α), play a role in the early evolutionary stages of experimental acute GVHD. In the anti-minor H antigen GVHD model elicited by CD4$^+$ effector T cells, marked degranulation of mast cells and associated dyskeratosis of keratinocytes characterized the early evolutionary stages of disease and preceded the influx of effector lymphocytes. Degranulation of mast cells was first

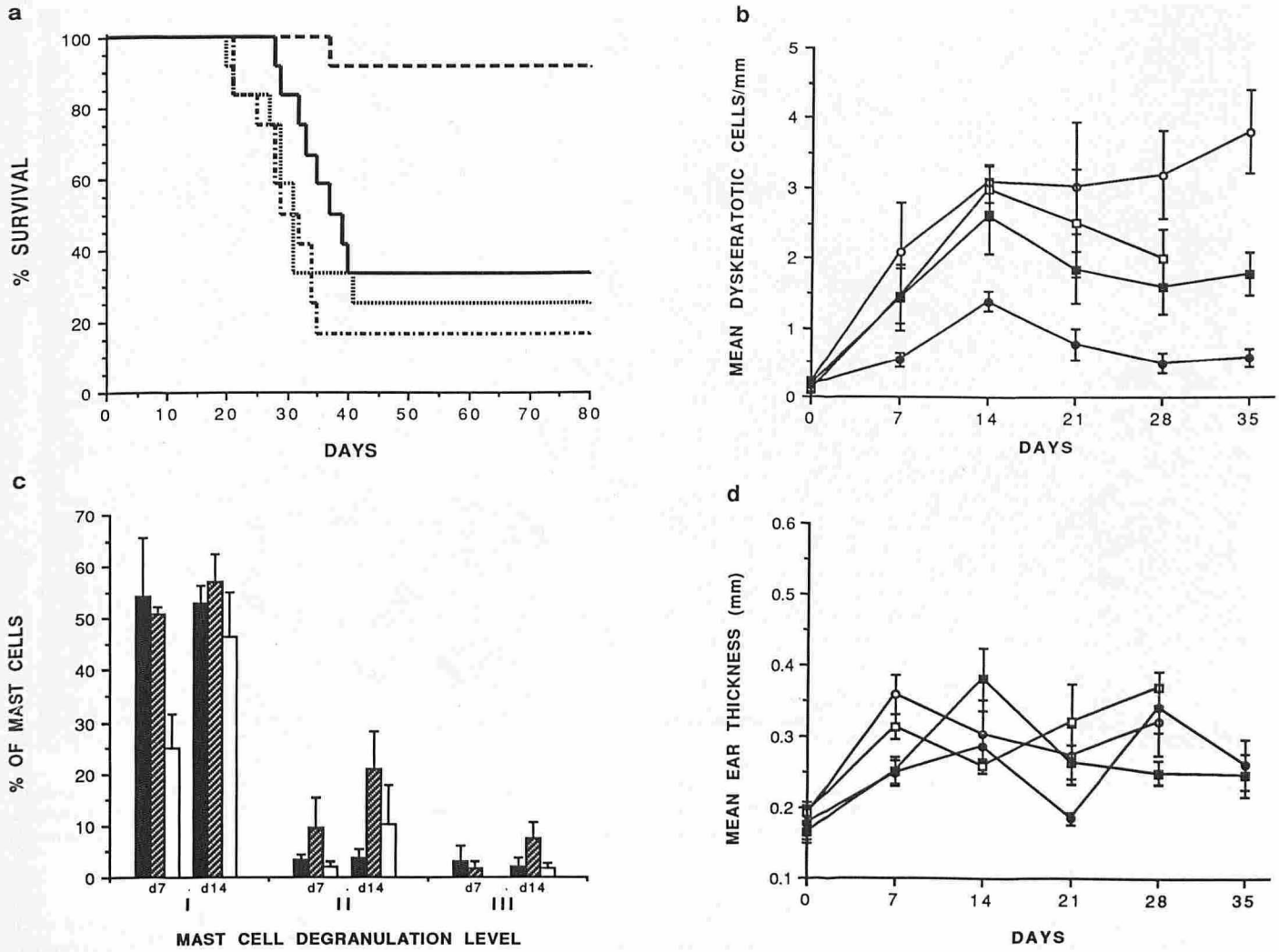

Figure 4. Effect of anti-TNF-α Ab on development of CD8$^+$ T-cell-mediated GVHD. *a)* Survival and incidence of GVHD. CBA mice were irradiated (800 cGy) and injected intravenously with either 2×10^6 B10.BR ATBM cells alone (- - -; n = 14) or with 2.5×10^6 B10.BR CD8$^+$ T cells. The latter mice were divided into three groups, the first left untreated (——; n = 15), the second given anti-TNF-α Ab (2 mg intravenously, 1 h before cells were injected; 2 mg intraperitoneally weekly thereafter till day 42) (·-·-·-·-· ; n = 18), and the third treated with control CFA RIgG (2 mg intravenously, 1 h before cells were injected; 2 mg intraperitoneally weekly thereafter till day 42) (····· ; n = 16). *b)* Sequential analysis of the mean ± SEM number of dyskeratotic cells/linear mm of skin from CBA mice of the four groups described in *(a)* from days 0–35 post-transplantation; *n* = 3 for untreated (-O-), anti-TNF-α Ab (□), CFA RIgG (■), and ATBM (●) groups. *c)* The mean ± SEM percentage of mast cells degranulating and the extent of degranulation in the skin of CBA mice from the untreated (■), anti-TNF-α Ab treated (▨), and ATBM (□) groups at days 7 and 14 post-transplantation (n = 3 for all groups). *d)* Sequential analysis of the mean ± SEM ear thickness from CBA mice of the four groups described in *(b)* from days 0–35 post-transplantation (n = 3 for all groups and timepoints).

demonstrable at day 7 post-transplantation, whereas by day 14, notable intravascular accumulation of leukocytes and extravasation of lymphocytes, followed by exocytosis and focal satellitosis in the epidermis, were observed. These findings suggest a temporal linkage between the degranulation of mast cells and early epidermal injury before the influx of effector CD4$^+$ lymphocytes, and is consonant with previous studies linking mast cell degranulation and TNF-α liberation to the influx of helper T cells [29]. Stuart and co-workers [30] have previously demonstrated that the number of mast cells significantly increased at early timepoints (days 6 and 8) in both DA and Brown-Norway rats undergoing GVHD induction, but significantly decreased at later timepoints. The observations in both the rat and the current murine models raises the possibility that a humoral factor produced by allostimulated effector cells may induce the proliferation, activation, and degranulation of mast cells in the early phase of GVHD. Indeed, the production of "histamine-releasing factors" by activated T cells has been proposed to explain how mast cells are induced to degranulate during the early phase of delayed hypersensitivity reactions and in experimental chronic GVHD [31]. In our model, such humoral factors would be expected to be produced in extracutaneous sites at day 7, because lymphocytes were not observed in lesional skin at this juncture. By day 14 and beyond, when inflammatory cells infiltrate skin, both systemic as well as locally produced factors could facilitate mast cell degranulation.

The temporal relationship observed in this study between mast cell degranulation and dyskeratosis would suggest that soluble factors (cytokine/s) released during the process of degranulation might contribute to keratinocyte injury. TNF-α is one such candidate to mediate this effect, as it appears to be produced and released by activated murine mast cells [11–13]. Similar observations have been made in our own laboratory with human skin samples, indicating that a) TNF-α is predominantly synthesized, stored, and released by dermal mast cells; b) keratinocytes and dermal monocytes express very little constitutive TNF-α by comparison; and c) based on ultrastructural and immunohistochemical evidence, mast cell degran-

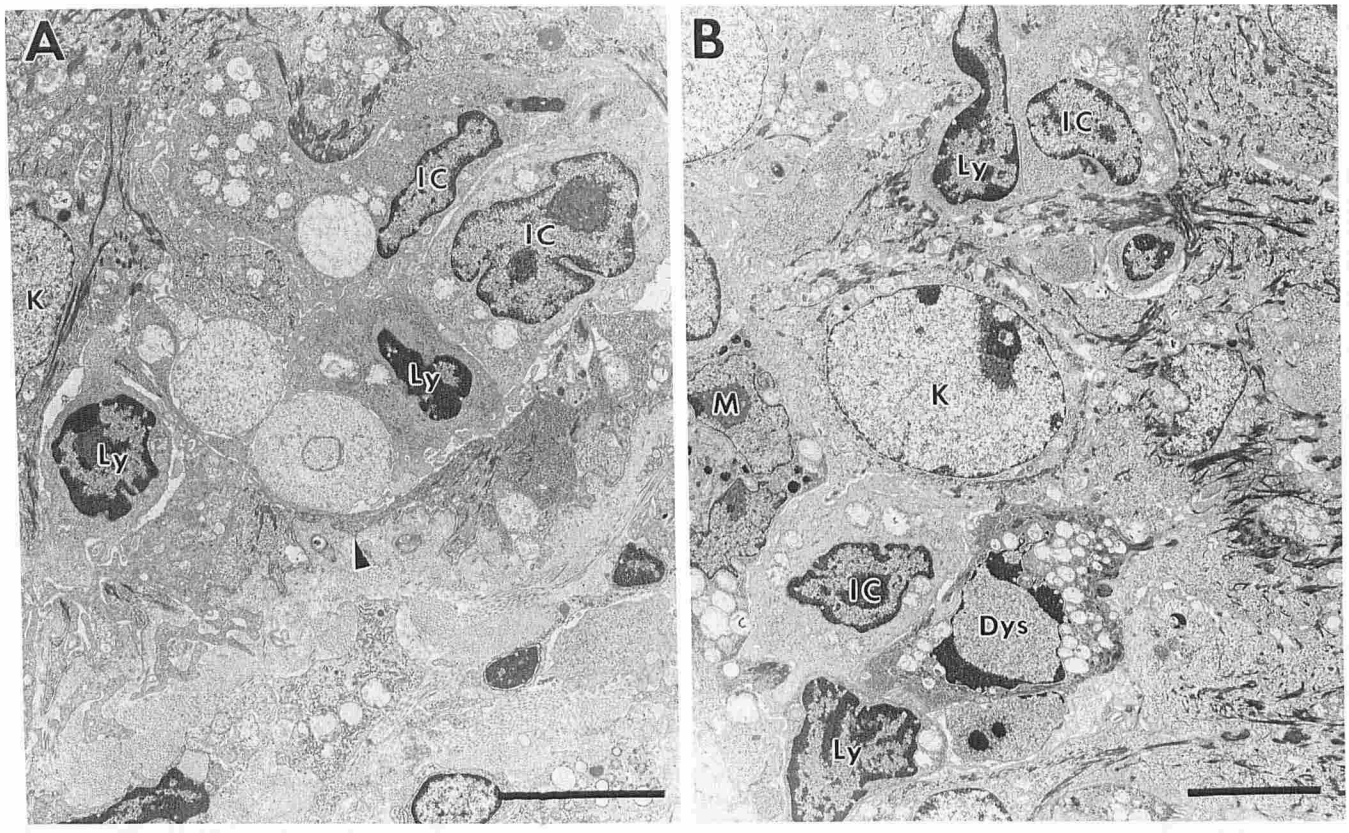

Figure 5. Electron micrographs of exocytosis and satellitosis in CD4+ cell-mediated GVHD (days 14–28). *A)* Lymphocytes (Ly) and indeterminate mononuclear cells (IC) are aggregated within the lower layers of the epidermis where the majority of epidermal injury is noted. K, keratinocyte; *arrowhead,* dermal-epidermal junction (*bar,* 5 μm). *B)* Several indeterminate mononuclear cells and lymphocytes are grouped around dyskeratotic cell (Dys), evidence of "satellitosis." M, melanocyte (*bar,* 5 μm).

ulation closely correlates with released amounts of TNF-α [14]. In regard to the potential involvement of TNF-α in dyskeratosis, cytostatic effects of either TNF-α, lymphotoxin, or gamma interferon (IFN-γ) on cultured human keratinocytes have been reported [6,32]. These cytokines independently inhibit human keratinocyte DNA synthesis and the combined treatment with either TNF-α or lymphotoxin and IFN-γ enhances keratinocyte cytostasis (although not necessarily necrosis/dyskeratosis) and after 2–3 d leads to exaggerated changes in cell morphology [6]. In addition, preliminary data (Murphy and Tharp, unpublished) suggest that TNF-α in combination with certain mast cell enzymes, such as chymase, are toxic to human keratinocytes *in vitro.* These findings, along with recent evidence that IFN-α, -β, and -γ upregulate TNF-α receptors fit, perhaps, with a contributing role for TNF-α in the development of epidermal GVHD [33].

Table I. Summary of Morphologic Findings in CD4+ and CD8+ Mediated Acute GVDH

	CD4+	CD8+
Mast cell degranulation		
Severity	Early (day 7), moderate–severe	Early (day 7), mild
Extent	More focal	More diffuse
Dyskeratosis	Present (before leukocytic infiltration)	Present (before leukocytic infiltration)
Endothelium	Activated phenotype (by day 14)	Activated phenotype (by day 14)
Neutrophils	Intralumenal (day 14)	None observed
Lymphocytes	Gradual increase (days 14–35)	Gradual increase (days 14–35)
Epidermotrophism	Prominent	Less prominent
Satellitosis	Variable[a]	Variable[a]

[a] The designation "variable" indicates that not all epidermotrophic lymphocytes were in apposition to degenerating or necrotic keratinocytes, nor were all degenerating or necrotic keratinocytes in apposition to epidermotropic lymphocytes.

Recent studies by Piguet and co-workers [5,7] have suggested a role for TNF-α in the epithelial alterations generated in a semi-allogeneic MHC murine GVHD model, based on the findings that the injection of anti–TNF-α IgG remarkably improved mortality and reduced the number of necrotic epidermal cells, although it failed to prevent T-cell activation and development of GVHD. They speculated that the source of TNF-α in GVHD must be related to cellular alterations in the dermis, such as from stimulated T lymphocytes [34], macrophages [35], and/or natural killer cells [36–38]. In the present study, although immunohistochemical confirmation is lacking, the consistent observation of infiltrating lymphocytes containing membrane-bound granules is consistent with our previous structural and immunocytochemical observations that large granular lymphocytes may play an important role in the effector phase of this disease [38].

The present study demonstrates that anti–TNF-α Ab treatment can significantly ameliorate mortality and reduce the number of dyskeratotic epidermal cells associated with a CD4+ T-cell–mediated GVHD response to minor H antigens. In addition to potential inhibition of direct TNF-α–mediated keratinocyte toxicity, the mechanism for this anti–TNF-α Ab treatment effect also may involve decreased recruitment and diapedesis of effector lymphocytes. For example, anti–TNF-α Ab treatment significantly diminished the ear thickness, a parameter that correlates closely with the quantity of cellular infiltration in this model. In human skin, TNF-α is known to induce endothelial adhesion molecules, such as E-selectin [14,39,40] and vascular cell adhesion molecule-1 (VCAM-1) [41], which may play a critical role in recruiting effector

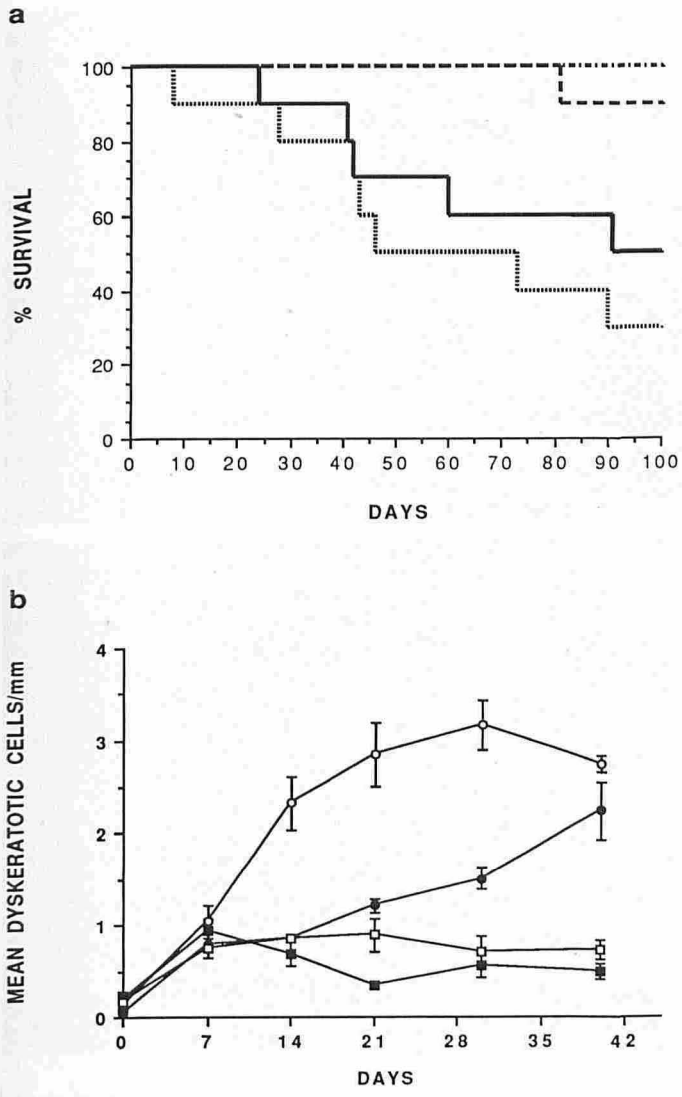

Figure 6. Effect of genetic mast cell depletion on CD8+ T-cell–mediated GVHD. *a)* Survival and incidence of GVHD. 2×10^6 C3H.SW ATBM cells were injected i.v. into irradiated (850 cGy) B6WW^V (- -) and B6$^{+/+}$ (-·-·-·-·-) mice, alone or with 4×10^6 C3H.SW CD8+ T cells (CD8→B6WW^V (——); CD8→B6$^{+/+}$ (·····); n = 10 for all groups. *b)* Sequential analysis of the mean ± SEM number of dyskeratotic cells/linear mm of skin from the four groups described in (*a*) from days 0–35 post-transplantation (n = 3 for all groups and timepoints). ATBM→B6WW^V (-■-), ATBM→B6$^{+/+}$ (-[ ]-). (CD8→B6WW^V (-●-), CD8→B6$^{+/+}$ (-○-).

leukocytes to the skin microvessels about which mast cells normally reside.

Aside from toxic effects on keratinocytes and induction of endothelial-leukocyte adhesion molecules, TNF-α may also contribute to the regulation and interaction of effector leukocytes and target cells in acute GVHD. Resting T cells do not normally express TNF-α receptors but they are inducible upon activation [42]. Once receptors are present, TNF-α can then enhance expression of the α subunit of the IL-2 receptor and can synergize with IL-2 with respect to both stimulation of T-cell proliferation and production of IFN-γ [42]. In turn, IFN-γ can upregulate TNF-α receptors, among other surface molecules, and increase the target cell susceptibility to TNF-α–mediated cytotoxicity [43]. In addition TNF-α–induced production of other cytokines including IL-1 [44], IFN-β2/IL6 [45], IFN-β1 [46], and granulocyte macrophage-colony stimulating factor GM-CSF [47] may contribute to the activation of effector leukocytes and enhancement of the immune response. In the present study, the inability of anti–TNF-α pretreatment to inhibit dyskeratosis at day 7 in CD4+ T-cell–mediated disease suggests the possibility that factors other than, or in addition to, this cytokine (perhaps local mast cell proteases or circulating systemic factors) may contribute to these early alterations. On the other hand, the efficacy of this treatment at later timepoints associated with leukocyte infiltration raises the possibility that TNF-α is primarily important for the trafficking of effector lymphocytes to prospective target sites and for the modulation of direct effector-target cell interactions. At these later timepoints, anti–TNF-α Ab treatment may inhibit TNF (either -α or -β, because both antisera and MoAb generated to TNF-α crossreact with TNF-β [48]) produced from a variety of cellular sources, including mast cells, keratinocytes, monocyte/macrophages, and by effector lymphocytes that migrate into the epidermis, where they are spatially associated with target epithelial cells.

In the B10.BR → CBA GVHD model elicited by CD8+ effector cells, the early phase was characterized by mast cells that exhibited a low number of granules but were devoid of ultrastructural evidence of degranulation in comparison to those cells found in CD4+ cell-mediated disease. We currently do not know the significance of these hypogranulated mast cells, although it seems likely that they may represent previously degranulated cells not "captured" in the timepoint examined. In contrast to CD4+ T-cell–mediated GVHD, the present study suggests that TNF-α is irrelevant to epithelial injury and inflammatory events in CD8+ T-cell–mediated GVHD development. The basis for this notion is that anti–TNF-α Ab failed to affect either survival or the number of dyskeratotic cells in the skin at any timepoint. Interestingly, the previous observations of more extensive gut involvement in CD4+ T-cell–mediated GVHD in comparison to CD8 disease [30,49,50] raise the possibility that participation of TNF in the former may contribute to the observed differences in severity of target cell injury at this site.

The effect of genetic depletion of mast cells on CD8+ T-cell–mediated GVHD in the C3H.SW → B6WW^V strain combination can be summarized as a delay in disease onset that correlated with the appearance of granulated mast cells. This was marked by a significant prolongation of survival and a shift to later timepoints post-transplantation with regard to the development of intravascular accumulation and diapedesis of lymphocytes and an increased number of dyskeratotic cells, compared with the C3H.SW → B6$^{+/+}$ control strain combination. Eventual disease onset and progression in B6WW^V mice correlated with the appearance of granule-containing dermal mast cells at later timepoints. In B6WW^V mice, the fixed precursors of mast cells in the skin are markedly depleted [51] and bone marrow transplantation from B6$^{+/+}$ mice can dramatically increase the number of mast cells between 35–75 d post-transplantation [52]. The *W* locus has been shown to be allelic with the c-*kit* proto-oncogene and encodes for a protein that is a member of the transmembrane tyrosine kinase receptor family [53,54]. Therefore, it is likely that the recovery of mast cells in transplanted B6WW^V mice is due to the proliferation and differentiation of precursor cells from the donor bone marrow [51,55]. Alternatively, B6WW^V mice may possess a few precursor mast cells in their skin that can be promoted to differentiate by donor-derived humoral factors or inducer cells without involving the c-*kit* pathway. Support for this notion has come from both *in vitro* stem cell proliferation experiments [56] and an *in vivo* model in which local development of a large number of mast cells at sites of idiopathic chronic dermatitis in B6WW^V mice, independent of bone marrow transplantation, has been reported [57]. In this case, the etiology of the chronic dermatitis that had developed in the B6WW^V mice was unknown and the authors suggested that putative growth factors produced in the course of disease might participate in the local development of mast cells.

In conclusion, the present study suggests that factors released by degranulation of mast cells, elicited by both CD4+ and CD8+ effector T cells in the initial phases of GVHD, play an important role in

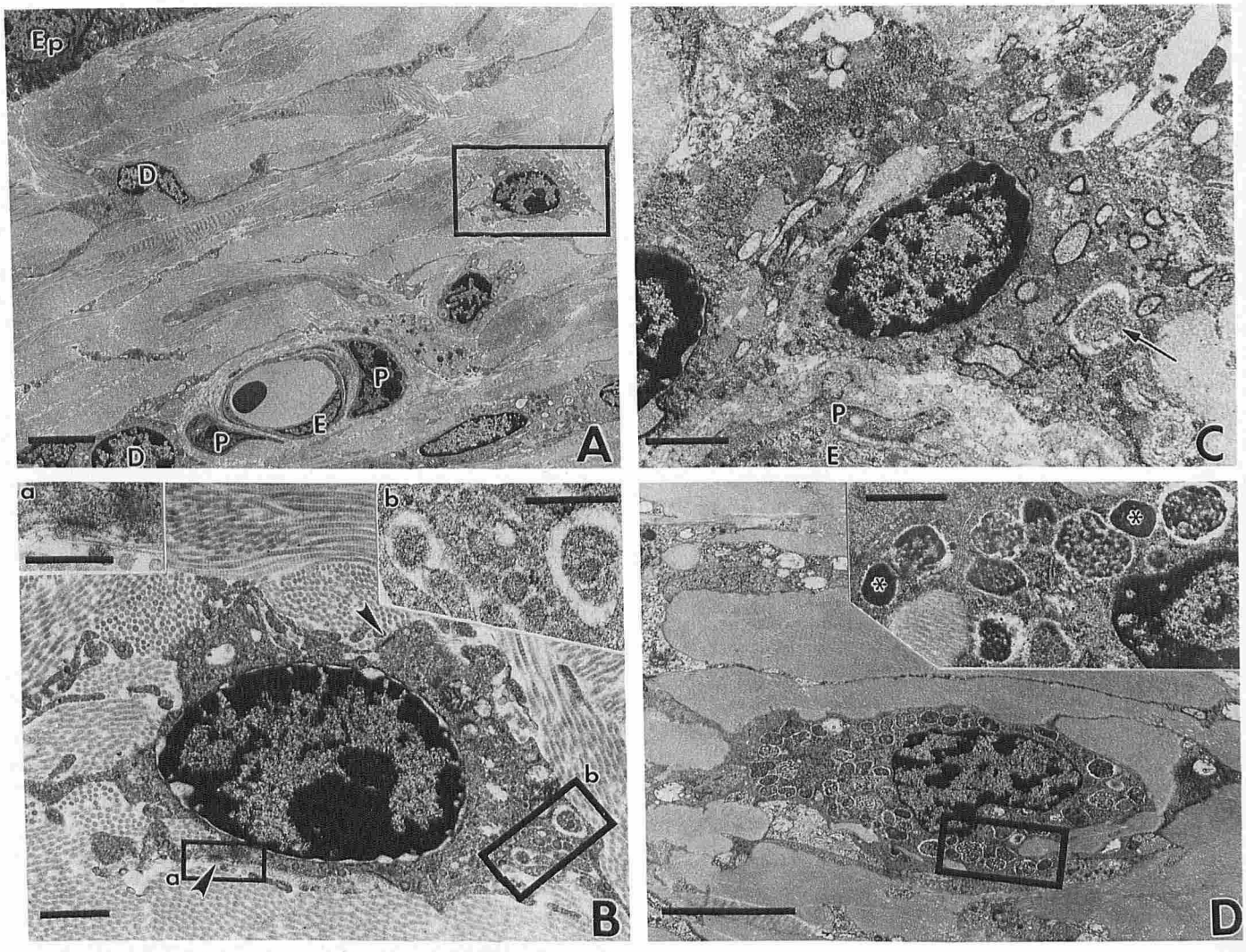

Figure 7. Ultrastructural analysis of mast cells in B6WW^v mice. *A)* Mononuclear cells devoid of mast cell granules *(rectangular area)* were observed around dermal microvessels at the time of transplantation (day 0). Ep, epidermis; D, dermal dendrocyte; P, pericyte; E, endothelial cell (*bar,* 5 μm). *B)* High power view of agranular mononuclear cells depicted in *rectangular area* of *(A)*. These cells displayed dendritic cytoplasmic processes and contained poorly defined cytoplasmic vesicles, fibronexus-like electron-dense plaques (*arrowheads,* high power view shown in inset *(A)*; *bar,* 0.5 μm), and occasional vacuoles containing moderately electron-dense granular material (*bar,* 1 μm). High power view of the *rectangular area b* is shown in (*B; bar,* 0.5 μm). *C)* Mononuclear cell around microvessel on day 14 exhibits marked widening of rough endoplasmic reticulum and moderately electron-dense granular matrices *(arrow)*. P, pericyte; E, endothelial cell (*bar,* 1 μm). *D)* A definitive mast cell on day 40, which contained some electron-dense granules *(asterisks)* and moderately degranulated matrices (×4,000; *bar,* 5 μm). *Inset,* high power view of rectangular area (*bar,* 1 μm).

early epithelial injury that is independent of direct contact with donor lymphocytes. The administration of anti-TNF-α Ab to recipient mice failed to abrogate this early injury in both types of GVHD, but could diminish the level of injury at later timepoints in $CD4^+$ T-cell-mediated disease. Dermal mast cells may still play a critical role in the early and direct development of dyskeratosis, and may also be important in indirectly facilitating effector cell trafficking *via* endothelial activation. At least in $CD8^+$ T-cell-mediated GVHD, the presence of mast cells appears to be required for the development of disease. Overall, these findings suggest that the potential clinical application of anti-TNF-α Ab treatment for patients with severe acute GVHD may have limited value, and may be most effective in decreasing skin and gut lesions induced by $CD4^+$ alloreactive T cells. The results of a recent clinical pilot study with anti-TNF-α Ab treatment is consistent with this notion, in that although in the majority of cases the treatment was ineffective in preventing GVHD-related fatality, beneficial responses were found predominantly in the gut and skin [58]. We speculate that suppression of mast cell activity, in general, may have an even broader effect on the development and natural progression of GVHD.

This work was supported by United Public Health Service Grants CA-38951, HD-21926, CA-40358, and CA-38355 from the National Institutes of Health.

REFERENCES

1. Santos GW, Hess AD, Vogelsang GB: Graft-versus-host reactions and disease. *Immunol Rev* 88:169-192, 1985
2. Sale GE, Shulman HM, McDonald GB, Shulman HM, Thomas ED: Gastrointestinal graft-versus-host disease in man. A clinicopathological study of the rectal biopsy. *Am J Surg Pathol* 3:291-299, 1979
3. Volc-Platzer B, Rappersberger K, Mosberger I, Hinterberger W, Emminger-Schmidmeier W, Radaszkiewicz T, Wolff K: Sequential immunohistologic analysis of the skin following allogeneic bone marrow transplantation. *J Invest Dermatol* 91:162-168, 1988
4. Cohen J: Cytokines as mediator of graft-versus-host disease. *Bone Marrow Transplant* 3:193-197, 1988
5. Piguet PF, Grau GE, Allet B, Vassalli P: Tumor necrosis factor/cachectin is an effector of skin and gut lesions of the acute phase of graft-vs.-host disease. *J Exp Med* 166:1280-1289, 1987
6. Symington FW: Lymphotoxin, tumor necrosis factor, and gamma interferon are cytostatic for normal human keratinocytes. *J Invest Dermatol* 92:798-805, 1989
7. Piguet PF: Tumor necrosis factor and graft-vs.-host disease. In: Burakoff SJ, Deeg HJ, Ferrara JLM, Atkinson K (eds.). *Graft-Versus-Host Disease: Immunology,*

Pathophysiology, and Treatment. Marcel Dekker Inc, New York, pp 255–276, 1990
8. Ihle JN, Keller J, Oroszlan S, Henderson LE, Copeland TD, Fitch FW, Prystowsky MB, Goldwasser E, Schrader JW, Palszynski E, Dy M, Lebel B: Biological properties of homogeneous interleukin 3. I. Demonstration of WEHI-3 growth factor activity, mast cell growth factor activity, P cell-stimulating factor activity, colony-stimulating factor activity, and histamine-producing cell-stimulating factor activity. *J Immunol* 131:282–287, 1983
9. Gajewski TF, Fitch FW: Anti-proliferative effect of IFN-g in immune regulation. IV. Murine CTL clones produce IL-3 and GM-CSF, the activity of which is masked by the inhibitory action of secreted IFN-*γ*. *J Immunol* 144:548–556, 1990
10. Claman HN, Lee Choi K, Sujansky W, Vatter AE: Mast cell "disappearance" in chronic murine graft-vs-host disease (GVHD)-ultrastructural demonstration of "phantom mast cells." *J Immunol* 137:2009–2013, 1986
11. Jadus MR, Schmunk G, Djeu JY, Parkman R: Morphology and lytic mechanisms of interleukin 3-dependent natural cytotoxic cells: tumor necrosis factor as a possible mediator. *J Immunol* 137:2774–2783, 1986
12. Young JD, Liu CC, Butler G, Cohn ZA, Galli SJ: Identification, purification, and characterization of a mast cell-associated cytolytic factor related to tumor necrosis factor. *Proc Natl Acad Sci USA* 84:9175–9179, 1987
13. Richards AL, Okuno T, Takagaki Y, Djeu JY: Natural cytotoxic cell-specific cytotoxic factor produced by IL-3-dependent basophilic/mast cells. Relationship to TNF. *J Immunol* 141:3061–3066, 1988
14. Walsh LJ, Trinchieri G, Waldorf HA, Whitaker D, Murphy GF: Human dermal mast cells contain and release tumor necrosis factor *α*, which induces endothelial leukocyte adhesion molecule 1. *Proc Natl Acad Sci USA* 88:4220–4224, 1991
15. Obleid LM, Linardic CM, Karolak LA, Hannun YA. Programmed cell death induced by ceramide. *Science* 259:1769–1771, 1993
16. Cheng J, Turksen Q-C, Schreiber H, Teng M, Fuchs E. Cachexia and graft-vs.-host-disease-type skin changes in keratin promoter-driven TNFa transgenic mice. *Genes Devel* 6:1444–1456, 1992
17. Korngold R, Sprent J: Lethal graft-versus-host disease following bone marrow transplantation across minor histocompatibility barriers in mice. Prevention by removing mature T cells from marrow. *J Exp Med* 148:1687–1698, 1978
18. Korngold R, Sprent J: Variable capacity of L3T4$^+$ T cells to cause graft-versus-host disease across minor histocompatibility barriers in mice. *J Exp Med* 165:1552–1564, 1987
19. Hamilton BL: L3T4-positive T cells participate in the induction of graft-vs-host disease in response to minor histocompatibility antigens. *J Immunol* 139:2511–2515, 1987
20. Ferrara JLM, Marion A, McIntyre JF, Murphy GF, Burakoff SJ: Amelioration of acute graft vs host disease due to minor histocompatibility antigens by in vivo administration of anti-interleukin 2 receptor antibody. *J Immunol* 137:1874–1877, 1986
21. Ferrara J, Guillen FJ, Sleckman B, Burakoff SJ, Murphy GF: Cutaneous acute graft-versus-host disease to minor histocompatibility antigens in a murine model: histologic analysis and correlation to clinical disease. *J Invest Dermatol* 86:371–375, 1986
22. Ferrara JLM, Guillen FJ, Van Dijken PJ, Marion A, Murphy GF, Burakoff SJ: Evidence that large granular lymphocytes of donor origin mediate acute graft-versus-host disease. *Transplant* 47:50–54, 1989
23. Murphy GF, Whitaker D, Sprent J, Korngold R: Characterization of target injury of murine acute graft-*versus*-host disease directed to multiple minor histocompatibility antigens elicited by either CD4$^+$ or CD8$^+$ effector cells. *Am J Pathol* 138:983–990, 1991
24. Bruce J, Symington FW, Mckearn TJ, Sprent J: A monoclonal antibody discriminating between subsets of T and B cells. *J Immunol* 127:2496–2501, 1981
25. Dialynas DP, Wilde DB, Marrack P, Pierres A, Wall KA, Havran W, Otten G, Loken MR, Pierres M, Kappler J, Fitch FW: Characterization of the murine antigenic determinant designated L3T4a, recognized by monoclonal antibody GK1.5: Expression of L3T4a by functional T cell clones appears to correlate primarily with class II MHC antigen reactivity. *Immunol Rev* 74:29–56, 1983
26. Ceredig R, Lowenthal J, Nobholz M, McDonald HR: Expression of interleukin-2 receptors as a differentiation marker on intrathymic stem cells. *Nature* 314:98–100, 1985
27. Sarmiento M, Glasebrook AL, Fitch FW: IgG or IgM monoclonal antibodies reactive with different determinants on the molecular complex bearing Lyt 2 antigen block T cell-mediated cytolysis in the absence of complement. *J Immunol* 125:2665–2672, 1980
28. Teuscher C, Hickey WF, Korngold R: An analysis of the role of tumor necrosis factor in the phenotypic expression of activity induced experimental allergic orchitis and experimental allergic encephalomyelitis. *Clin Immunol Immunopathol* 54:442–453, 1990
29. Waldorf HA, Walsh LJ, Schechter NM, Murphy GF: Early cellular events in evolving cutaneous delayed hypersensitivity in humans. *Am J Pathol* 138:477–486, 1991
30. Stuart SP, Klein RM, Clancy Jr J: Kinetics of mast cell, fibroblast, and epidermal cell proliferation during acute graft-versus-host disease in the neonatal rat. *J Invest Dermatol* 88:369–374, 1987
31. Levi-Schaffer F, Mekori YA, Segal V, Claman HN: Histamine release from mouse and rat mast cells cultured with supernatants from chronic murine graft-vs-host splenocytes. *Cell Immunol* 127:146–158, 1990
32. Pillai S, Bikle DD, Eessalu TE, Aggarwal BB, Elias PM: Binding and biological effects of tumor necrosis factor alpha on cultured human neonatal foreskin keratinocytes. *J Clin Invest* 83:816–821, 1989
33. Royo C, Jacquet S, Brandely M, Touraine JL: Effect of recombinant gamma interferon on the graft versus host reaction in mice. *Bone Marrow Transplant* 2:295–302, 1987
34. Cuturi MC, Murphy M, Costa-Giomi MP, Weinmann R, Perussia B, Trinchieri G: Independent regulation of tumor necrosis factor and lymphotoxin produced by human peripheral blood lymphocytes. *J Exp Med* 165:1581–1594, 1987
35. Higuchi H, Higashi N, Taki H, Osawa T: Cytolytic mechanism of activated macrophages. Tumor necrosis factor and L-arginine-dependent mechanisms act synergically as the major cytolytic mechanisms of activated macrophages. *J Immunol* 144:1425–1431, 1990
36. Delgliantoni G, Murphy M, Kobayashi M, Francis M-K, Perussia B, Trichieri G: Natural killer (NK) cell-derived hematopoietic colony-inhibiting activity and NK cytotoxic factor. Relationship with tumor necrosis factor and synergism with immune interferon. *J Exp Med* 162:1512–1530, 1985
37. Acevedo A, Aramburn J, Fernandez-Herrera J, Fernandez-Ranada JM, Lopez-Botet: Identification of natural killer (NK) cells in lesions of human cutaneous graft-versus-host disease: expression of novel NK-associated surface antigen (kp43) in mononuclear infiltrates. *J Invest Dermatol* 97:659–666, 1991
38. Guillen F, Ferrara J, Hancock WW, Messadi D, Fonferko E, Burakoff SJ, Murphy GF: Acute cutaneous graft-versus-host disease to minor histocompatibility antigens in a murine model. Evidence that large granular lymphocytes are effector cells in the immune response. *Lab Invest* 55:35–42, 1986
39. Bevilacqua MP, Pober JS, Mendick DL, Cotrn RS, Gimbrone MAJr: Identification of an inducible endothelial-leukocyte adhesion molecule. *Proc Natl Acad Sci USA* 84:9238–9242, 1987
40. Klein LM, Lavker RM, Matis WL, Murphy GF: Degranulation of human mast cells induces an endothelial antigen central to leukocyte adhesion. *Proc Natl Acad Sci USA* 86:8972–8976, 1989
41. Osborn L, Hession C, Tizard R, Vassallo C, Luhowskyj S, Chi-Rosso G, Lobb R: Direct expression of cloning of vascular cell adhesion molecule 1, a cytokine-induced endothelial protein that binds lymphocytes. *Cell* 59:1203–1211, 1989
42. Scheurich P, Thoma B, Ucer U, Pfizenmaier K: Immunoregulatory activity of recombinant human tumor necrosis factor (TNF)-*α*: induction of TNF receptors on human T cells and TNF-*α* mediated enhancement of T cell responses. *J Immunol* 138:1786–1790, 1987
43. Royo C, Jacquet S, Brandely M, Touraine JL: Effect of recombinant gamma interferon on the graft versus host reaction in mice. *Bone Marrow Transplant* 2:295–302, 1987
44. Dinarello CA, Cannon JG, Wolff SM, Bernheim HA, Beutler B, Cerami A, Figari IS, Palladino MAJr, O'Connor JV: Tumor necrosis factor (cachectin) is an endogenous pyrogen and induces production of interleukin 1. *J Exp Med* 163:1433–1450, 1986
45. Zhang Y, Lin J-X, Vilcek J: Interleukin-6 induction by tumor necrosis factor and interleukin-1 in human fibroblasts involves activation of nuclear factor binding to a kb-like sequence. *Mol Cell Biol* 10:3818–3823, 1990
46. Jacobsen H, Mestan J, Mittnacht S, Dieffenbach CW: Beta interferon subtype 1 induction by tumor necrosis factor. *Mol Cell Biol* 9:3037–3042, 1989
47. Munker R, Gasson J, Ogawa M, Koeffler HP: Recombinant human TNF induces production of granulocyte-monocyte colony-stimulating factor. *Nature (London)* 323:79–82, 1986
48. Sheehan KC, Ruddle NH, Schreiber RD: Generation and characterization of hamster monoclonal antibodies that neutralize murine tumor necrosis factors. *J Immunol* 142:3884–3893, 1989
49. Guy-Grand D, Vassalli P: Gut injury in mouse graft-versus-host reaction: study of its occurrence and mechanisms. *J Clin Invest* 77:1584–1595, 1986
50. Mowat AM, Sprent J: Induction of intestinal graft-versus-host reactions across mutant major histocompatibility antigens by T lymphocyte subsets in mice. *Transplant* 47:857–863, 1989
51. Matsuda H, Kitamura Y, Sonoda T, Imori T: Precursor of mast cells fixed in the skin of mice. *J Cell Physiol* 108:409–415, 1981
52. Kitamura Y, Go S, Hatanaka K: Decrease of mast cell in *WW^V* mice and their increase by bone marrow transplantation. *Blood* 52:447–452, 1978
53. Chabot B, Stephenson DA, Chapman VM, Besmer P, Bernstein A: The proto-oncogene c-kit encoding a transmembrane tyrosine kinase receptor maps to the mouse W locus. *Nature* 335:88–89, 1988
54. Geissler EN, Ryan MA, Housman DE: The dominant-white spotting (W) locus of the mouse encodes the c-kit proto-oncogene. *Cell* 55:185–192, 1988
55. Hatanaka K, Kitamura Y, Nishimune Y: Local development of mast cells from bone marrow-derived precursors in the skin of mice. *Blood* 53:142–147, 1979
56. Kodama H, Nose M, Yamaguchi Y, Tsunoda J, Suda T, Nishikawa S, Nishikawa S: In vitro proliferation of primitive hemopoietic stem cells supported by stromal cells: evidence for the presence of a mechanism(s) other than that involving c-kit receptor and its ligand. *J Exp Med* 176:351–361, 1992
57. Galli SJ, Arizono N, Murakami T, Dvorak AM, Fox JG: Development of large numbers of mast cells at sites of idiopathic chronic dermatitis in genetically mast cell-deficient WBB6F1-*WW^V* mice. *Blood* 69:1661–1666, 1987
58. Hervé P, Flesch M, Tiberghien P, Wijdenes J, Racadot E, Bordigoni P, Plouvier E, Stephan JL, Bourdeau H, Holler E, Lioure B, Roche C, Vilmer E, Demeocq F, Kuentz M, Cahn JY: Phase I-II trial of a monoclonal anti-tumor necrosis factor a antibody for the treatment of refractory severe acute graft-versus-host disease. *Blood* 79:3362–3368, 1992